Eighth International Conference on
THIN-WALLED STRUCTURES – ICTWS 2018
Lisbon, Portugal, July 24-27, 2018

EFFECT OF IMPERFECTIONS AND RESIDUAL STRESSES ON THE SHEAR BUCKLING STRENGTH OF CORRUGATED WEB GIRDERS

D. Kollár* and B. Kövesdi*

* Budapest University of Technology and Economics, Department of Structural Engineering
e-mails: kollar.denes@epito.bme.hu, kovesdi.balazs@epito.bme.hu

Keywords: Geometric imperfection; Residual stress; Corrugated web girder; Shear buckling strength.

Abstract. *Application of steel I-girders with corrugated webs has been significantly increased in the past decades, especially in bridges. However, there are numerous unknown specialties in their structural behaviour compared to conventional I-girders with flat webs, which needs further investigations. Previously, a large number of test results and numerical simulations showed that the shear buckling resistance of corrugated web girders with slender webs is sensitive for imperfections due to residual stresses and initial geometric imperfections. However, the residual stress distribution of corrugated web girders has not been investigated previously in a detailed manner. The current paper introduces the finite element model of corrugated web girders developed for welding simulation. The developed numerical model is capable of simulating thermal phenomena during welding, and to determine residual stresses and manufacturing imperfections depending on welding variables. Welding-induced residual stresses and geometric imperfections and their effect on shear buckling behaviour and resistance are determined and discussed in the current paper.*

1 INTRODUCTION

Recently, the application of sinusoidal and trapezoidal corrugated profiles has increased in civil engineering structures. Corrugation is intended to increase the buckling resistance, thus, transverse stiffeners can be eliminated or their number can be significantly reduced. In addition, corrugated profiles are stiffer during construction, while automation of fabrication leads to a sustainable structure. The 'accordion effect' due to negligible axial stiffness and the normal stress distribution of corrugated web girders are well known in the design practice. Generally, standards only take the contribution of flanges into account in the calculation of bending moment resistance, while the corrugated web resists the shear force. Numerous investigations can be found in the international literature [1-8] dealing with shear buckling resistance of corrugated web girders, however, the influence of residual stresses and geometric imperfections due to the manufacturing process has not been analysed and clarified yet. The conjecture denotes that not even longitudinal normal stresses under axial loading or bending moment may be negligible in the web due to the 'accordion effect', but a similar phenomenon may occur in case of welding-induced residual stresses as well. The current study focuses on welding-induced imperfections and their effect on the shear buckling resistance, whilst the influence of cold-forming, thermal cutting is not taken into consideration. Basically, welding simulations are not generally used in civil engineering practice because of its complexity. However, it can provide useful information regarding the structural behaviour and resistance of steel structures, as shown in [9-12]. The current research program contains (i) literature review, (ii) experimental study of small scale test specimens, (iii) numerical investigation using finite element modelling for virtual manufacturing and testing and (iv) the evaluation of experimental and numerical results.

2 LITERATURE REVIEW

In general, the literature review focuses on the differences in residual stress models and shear buckling behaviour of corrugated web girders and conventional I-girders with flat webs. Deviations in structural behaviour are due to differences in manufacturing processes. Residual stress distributions due to cold-forming are not introduced in the current paper.

2.1 Residual stress models

There are numerous investigations dealing with residual stress distributions of welded I-sections and H-sections with conventional flat webs. These sections are widely used in civil engineering structures as beams, trusses and columns for a long while. Hence, investigations trended to residual stresses in the past decades to reveal the effect on structural resistance. Amongst others, Nagaraja, Estuar and Tall [13], Alpsten and Tall [14] were the leading researchers of residual stress measurements on welded I-sections using sectioning technique involving longitudinal saw cuts across the width and through the thickness of the components. Plenty of studies [15-19] dealt with longitudinal residual stress measurements of I-sections. Flame-cutting or milling of plates may have a large influence on residual stresses (Figure 1) and resistances, since longitudinal residual stresses become tensile on the edges that may increase the buckling strength. A couple of residual stress models have been developed for normal strength steel sections such as in ECCS [20], the Swedish standard [21], the Chinese standard [22], while models for residual stresses in high strength steel I-sections are also developed and published in [17] and [23]. The proposed longitudinal residual stress model by the ECCS and Swedish standard (BSK 99) is presented in Figure 1 representing a_{f1}, a_{f2}, a_{w1} and a_{w2} characteristic parameters for a bi-symmetrical I-section. ECCS recommends to use flange width and web height based parameters ($a_{f1} = 0.075b_f$, $a_{f2} = 0.125b_f$, $a_{w1} = 0.075h_w$ and $a_{w2} = 0.125h_w$), while the Swedish standard introduces plate thickness-dependent characteristic parameters ($a_{f1} = 0.75t_f$, $a_{f2} = 0.75t_f$, $a_{w1} = 1.5t_w$ and $a_{w2} = 3t_w$). However, it has to be emphasized that the Swedish code gives dimension limits (t_f and $t_w \leq 40$ mm, $b_f \geq 3t_f$ and $h_w \geq 6t_w$), while the ECCS recommendation is generally developed for S235 and S355 steel grades [18]. The σ_{cw} and σ_{cf} compressive membrane residual stresses in the web and flanges should be determined in conjunction with obtaining equilibrium of resultant internal forces. In general, these residual stress models neglect the variation of residual stresses through the thickness. However, Alpsten and Tall [14] drew attention that it may be taken into account when plate thickness is larger than 25 mm. Obviously, these models cannot be used for corrugated web girders, because corrugation results in an alternating shift of the tensile zone in the vicinity of the weld and thus compressive residual stresses will not be symmetrical in an arbitrary section. In addition, not even longitudinal normal stresses under axial loading or bending moment may be negligible in the web due to the ‘accordion effect’, but a similar phenomenon may occur in case of welding-induced residual stresses as well. Only several papers focus on residual stresses in corrugated web girders. Pasternak and Kubieniec [24] showed the highly nonlinear distribution of normal stresses in the flanges during bending tests using strain gauges. They concluded that the observed effect can be explained by the evidence of welding-induced residual stresses. Jáger et al. [25] and Lho et al. [26] introduced similar phenomenon by using indirect residual stress evaluation based on bending tests. Moon et al. [27] used a simplified residual stress model for flexural-torsional buckling calculations, although, the effect of eccentricities was not taken into account in compressive stresses and thus the resultant internal bending moment was not in equilibrium. To the best of the authors’ knowledge, results of transient thermal analysis or direct residual stress measurements have not been published for corrugated web girders, yet.

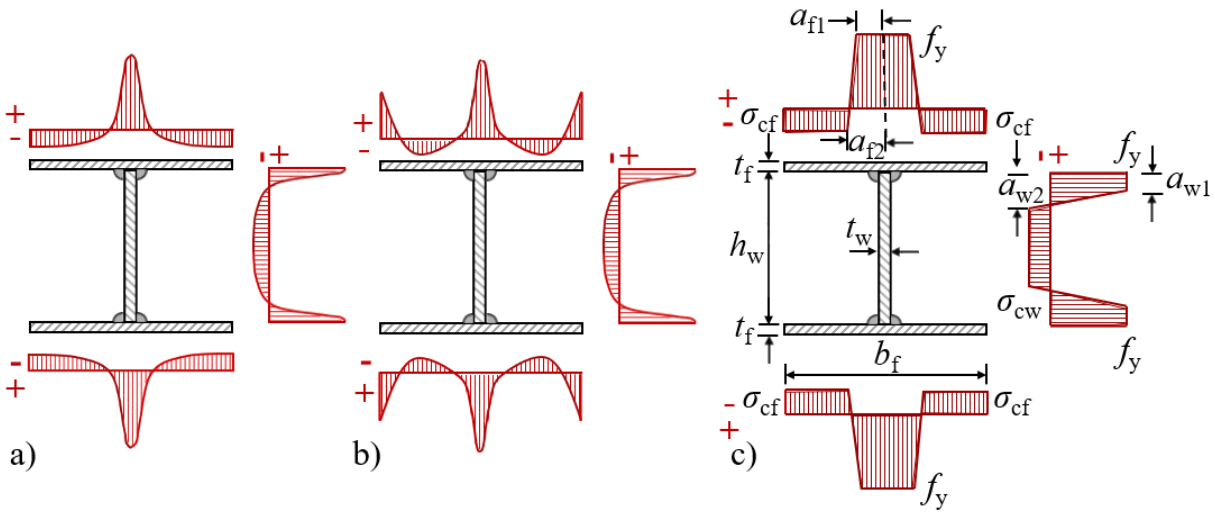

Figure 1: Welding-induced residual stresses a) using milling and b) flame-cutting on the edges; c) residual stress model of ECCS and BSK 99.

2.2 Design methods for shear buckling resistance

There are several design approaches for shear buckling strength calculation recommended by standards, technical reports and research papers. Eurocode [28] gives a design method for shear resistance calculation considering shear buckling at the ultimate limit state. First, recommendations for girders with flat webs (Equations 1-4) are presented to emphasize the differences in design approaches. $V_{b,Rd}$ denotes the design resistance for shear buckling including the contribution from the web ($V_{bw,Rd}$) and the flanges ($V_{bf,Rd}$) according to Equation 1. According to the standard, $V_{b,Rd}$ is limited by the plastic shear resistance of the web with a magnification factor of η (1.2 for steel grades up to S460 and 1.0 for higher steel grades).

$$V_{b,Rd} = V_{bw,Rd} + V_{bf,Rd} = \frac{\chi_w \, f_{yw} \, h_w \, t_w}{\sqrt{3}\,\gamma_{M1}} + \frac{b_f \, t_f^2 \, f_{yf}}{c\,\gamma_{M1}} \left(1 - \left(\frac{M_{Ed}}{M_{f,Rd}}\right)^2\right) \le \frac{\eta \, f_{yw} \, h_w \, t_w}{\sqrt{3}\,\gamma_{M1}} \tag{1}$$

$$c = a\left(0.25 + \frac{1.6 + b_f \, t_f^2 \, f_{yf}}{t \, h_w^2 \, f_{yw}}\right) \tag{2}$$

$$\overline{\lambda_w} = 0.76\sqrt{\frac{f_{yw}}{\tau_{cr}}} = 0.76\sqrt{\frac{f_{yw}}{k_\tau \, \sigma_E}} \tag{3}$$

$$\chi_w = \begin{cases} \overline{\lambda_w} < 0.83/\eta & \eta & \eta \\ 0.83/\eta \le \overline{\lambda_w} < 1.08 & 0.83/\overline{\lambda_w} & 0.83/\overline{\lambda_w} \\ \overline{\lambda_w} \ge 1.08 & 1.37/(0.7+\overline{\lambda_w}) & 0.83/\overline{\lambda_w} \end{cases} \tag{4}$$

Rigid end post | Non-rigid end post

Yield strengths of the web and flanges are denoted by f_{yw} and f_{yf}, respectively, while γ_{M1} is a partial safety factor if instability governs. Geometric notations are shown in Figure 2. The contribution from the flange depends on the bending moment M_{Ed} and the moment of resistance $M_{f,Rd}$ flanges. The parameter c takes the distance a between transverse stiffeners

into account (Equation 2). Non-dimensional slenderness $\overline{\lambda_w}$ of the web is calculated by Equation 3, where the shear buckling coefficient k_τ and Euler stress σ_E for a perfect plate can be found in Annex A in the EN 1993-1-5:2006 [28] to calculate critical shear stress τ_{cr}. The reduction factor χ_w is a function of rigid/non-rigid end post and the non-dimensional slenderness (Equation 4).

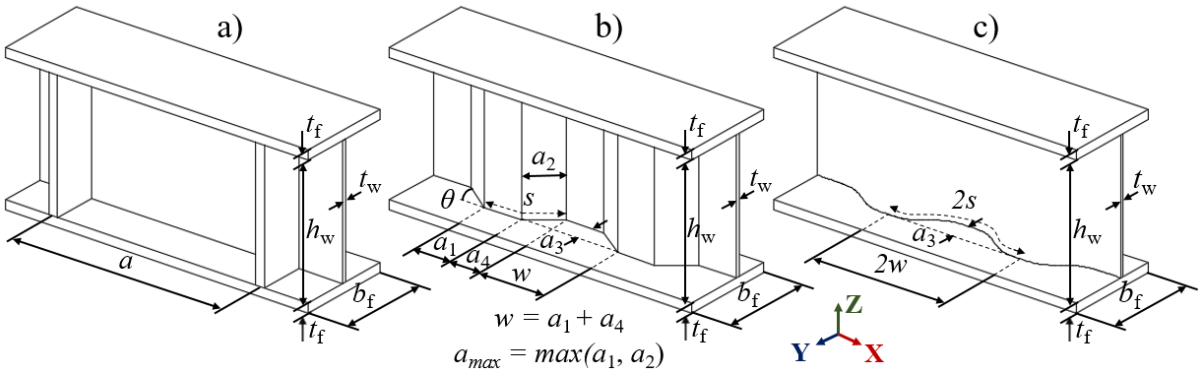

Figure 2: Geometric notations of typical a) conventional I-girders, b) trapezoidal and c) sinusoidal corrugated web girders.

Annex D of the EN 1993-1-5:2006 [28] gives design rules for trapezoidal and sinusoidal corrugated web girders. Geometric notations are shown in Figure 2. The shear buckling resistance is calculated using Equation 5 and it only takes the contribution of the web into account, while the influence of flanges is neglected. The reduction factor χ_c is the lesser of the values of reduction factors for local buckling $\chi_{c,l}$ and global buckling $\chi_{c,g}$ (Equations 6 and 7), while there is no recommendation in the code for taking interactive shear buckling into account. D_x and D_y are the longitudinal (x) and transverse (y) relative bending stiffness for a unit length of the web, respectively (Equation 8). I_z denotes the moment of inertia about the z axis of a half wave with a length of w, s is the unfolded length of a half wave, while E is Young's modulus and v is Poisson's ratio. The proposed design method is applicable for trapezoidal and sinusoidal corrugated web girders, although, the calculation of critical local shear stress $\tau_{cr,l}$ is different for sinusoidal and trapezoidal profiles.

$$V_{bw,Rd} = \frac{\chi_c \, f_{yw} \, h_w \, t_w}{\sqrt{3} \, \gamma_{M1}}, \quad \text{where} \quad \chi_c = \min\left(\chi_{c,l}, \chi_{c,g}\right) \tag{5}$$

$$\chi_{c,l} = \frac{1.15}{0.9 + \overline{\lambda_{c,l}}} \le 1.0, \quad \text{where} \quad \overline{\lambda_{c,l}} = \sqrt{\frac{f_{yw}}{\sqrt{3}\,\tau_{cr,l}}} \quad \text{and} \quad \tau_{cr,l} = 4.83E\left(\frac{t_w}{a_{\max}}\right)^2 \tag{6}$$

$$\chi_{c,g} = \frac{1.5}{0.5 + \overline{\lambda}_{c,g}^2} \le 1.0, \quad \text{where} \quad \overline{\lambda_{c,g}} = \sqrt{\frac{f_{yw}}{\sqrt{3}\,\tau_{cr,g}}} \quad \text{and} \quad \tau_{cr,g} = \frac{32.4}{t_w \, h_w^2} \sqrt[4]{D_x D_y^3} \tag{7}$$

$$D_x = \frac{E t_w^3}{12(1-v^2)} \frac{w}{s} \quad \text{and} \quad D_y = \frac{E I_z}{w} \tag{8}$$

In the field of corrugated web girders the first research activities focused on the global and local shear buckling resistance of corrugated web girders started in the '80s at Chalmers University of Technology according to Bergfelt and Leiva-Aravena [2]. Basically, the local elastic shear buckling stress [29] based on plate buckling theory and the global elastic shear buckling stress [30] using the orthotropic plate theory are the principles of all the formulae

and design approaches found in different standards and previous research papers. Several models [31]-[34] were proposed for local and global shear buckling, however, a research study by Leblouba et al. [35] demonstrated that the design formula found in EN 1993-1-5 [32] is more accurate for local and global shear buckling design. Leblouba et al. [36] presented a general formula (Equation 9) for critical interactive shear stress $\tau_{cr,i}$, where shear yield strength τ_y is equal to $f_{yw}/\sqrt{3}$ assuming von Mises yield criterion, while n and u are unitless parameters. For instance, the model by Sause and Braxtan [34] assumes $n = 3$ and $u = 2$. Leblouba et al. [36] also introduced the calculation of relative slenderness, normalized elastic shear buckling strength for local, global and interactive shear buckling. They proposed a new interactive model that performed better than the mentioned models in many aspects regarding a large experimental database.

$$\frac{1}{\tau_{cr,i}^{\ n}} = \frac{1}{\tau_{cr,l}^{\ n}} + \frac{1}{\tau_{cr,g}^{\ n}} + \frac{u}{\tau_{y}^{\ n}} \tag{9}$$

3 EXPERIMENTS

The aim of the experimental research program is to determine the typical welding-induced longitudinal residual stress distributions in different corrugated web girder configurations. Strain gauges are used on the corrugated webs during fabrication for the indirect analysis of transient thermal stresses. The strain gauges are placed quite far from the local heat sources, thus, only thermal and elastic strains are to be measured as plastic region is solely specific for the vicinity of the welds. The unloaded surfaces of the plates are in two-dimensional state of stress (i.e., plane stress). Thus, thermal and residual stresses cannot be calculated directly using the results of a single uniaxial strain gauge, the measured total strains are mainly used for the verification of the numerical model and not for the determination of the typical residual stress pattern. The determination of residual stresses is done indirectly using finite element simulations.

3.1 Experimental set-up

Nine I-girders with trapezoidal corrugated web are investigated in the experimental research program. 30 strain gauges are used for three specimens, while 10 strain gauges are applied for the remaining six specimens. Thus, 150 strain gauges are used altogether in the experimental research program. Strain gauges are situated on both sides of the web at the same position to measure the influence of welding-induced bending moment during manufacturing. The measurement system includes (i) KMT-LIAS-06-3-350-5EL uniaxial strain gauges with nominal resistance of 350 Ω (temperature limit between -40 °C and +95 °C), (ii) HBM Canhead amplifier systems, (iii) HBM MGCplus data acquisition system and (iv) a laptop for real-time visualization and saving to hard disk drive using the software catman Easy. A sampling rate of 10 Hz is applied during data acquisition. HBM Z70 cold curing adhesive is used for the strain gauge installation with temperature limit between -55 °C and +100 °C. The positions of strain gauges are shown in Figure 3, which were determined previously based on numerical simulations taking the temperature limit of strain gauges and adhesive into account.

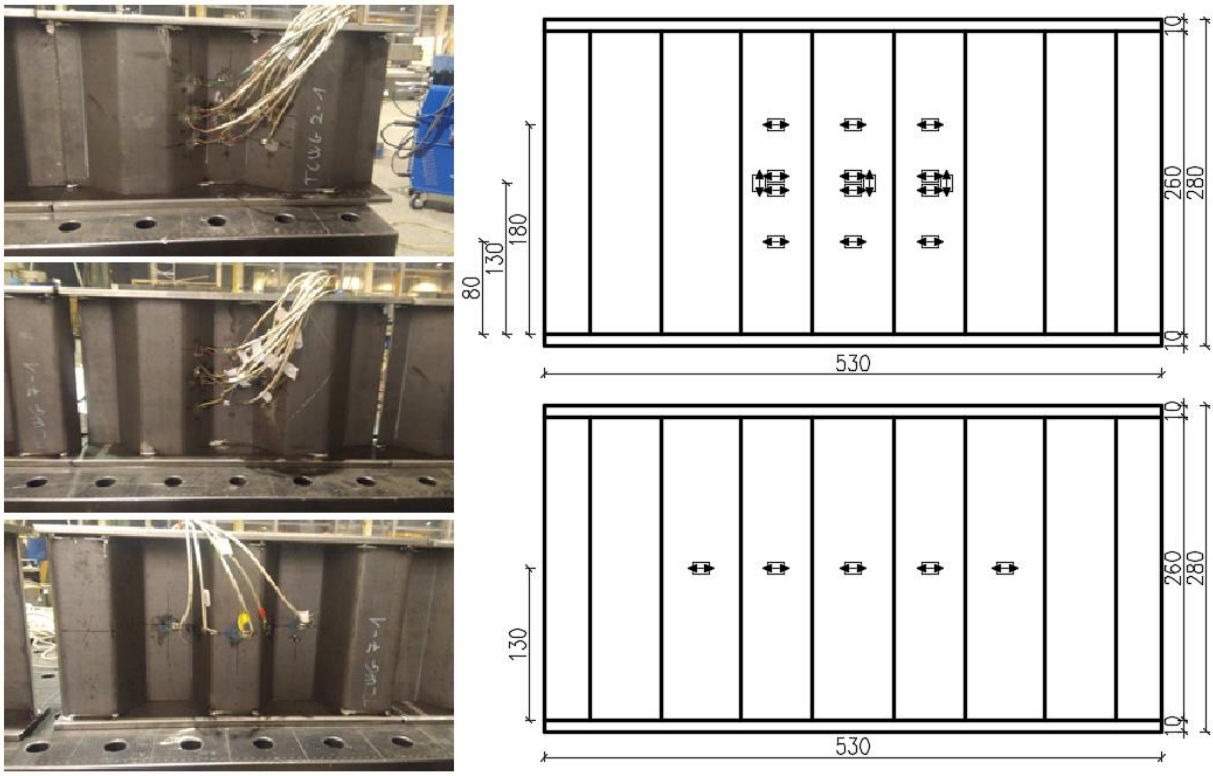

Figure 3: Corrugated web girders with strain gauges during the experiment and strain gauge positions for a 30-strain gauge and a 10-strain gauge case.

3.2 Specimens

The analysed configurations are presented in Figure 4. The applied corrugation angles are 30°, 45° and 60° for the three type of specimens, respectively. Three specimens are manufactured for each corrugation angle. All the specimens are made from S355 steel grade with a length of 530 mm and a height of 280 mm. Flanges are manufactured from steel plates with dimensions of 100 mm x 10 mm, with web thickness of 4 mm, and fold length is equal to 70 mm. Plasma cutting is used for carving the plates. Double-sided fillet welds are laid with throat thickness of 3 mm. A REHM Mega.Arc 450 welding power supply, M21 - ArC - 18 (Corgon 18) shielding gas and Böhler EMK 8 solid wire electrode with a diameter of 1.2 mm is used for metal active gas (135 MAG) welding during manufacturing. PB horizontal-vertical welding position is used for the fillet welds. Interpass temperature and the lengths of cooling phases are determined according to the measured temperatures at the strain gauge positions. The aim is to keep the temperature between 30-40 °C to limit the maximum temperatures of 90-100 °C at the strain gauges and thus avoid the deterioration of the joint between the web and the strain gauge. Greisinger GTH 1170 K type digital precision quick response thermometer is applied that makes temperature measurement possible for single material points. Ambient temperature was between 20-21 °C during the experiments. The applied nominal welding variables are the followings: voltage is 32.6 V, current is 259 A, while wire feed speed is 6 m/min. Travel speed is between 8.4-11.3 mm/s, °, 9.0-11.9 mm/s and 8.8-10.1 mm/s for specimens with corrugation angle of 30°, 45° and 60°, respectively. These inputs result in a total heat input per unit length of 7.5-10.0 kJ/cm, 7.1-9.4 kJ/cm and 8.3-9.6 kJ/cm, respectively. The 1st and 4th weld are welded in positive direction, while the 2nd and 3rd welds are welded in negative direction using a global coordinate system.

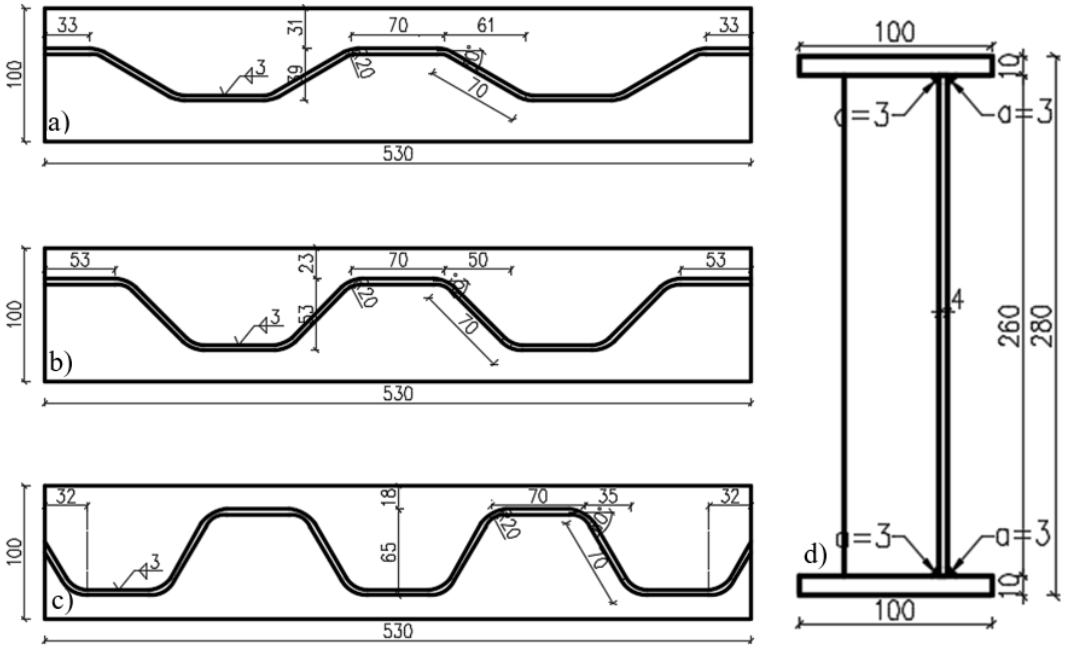

Figure 4: Specimen geometries with corrugation angle of a) 30°, b) 45° and c) 60°, while d) represents a typical cross section.

Experimental results are only used for verification purposes in the current paper, thus, the applied total strain vs. time curves are presented in 4.1.3 to verify the finite element model developed for welding simulation.

4 NUMERICAL MODEL

4.1 Welding simulation

4.1.1 Virtual manufacturing

Welding simulation of three different trapezoidal corrugated web girders are investigated using finite element analysis. The virtually manufactured specimens are identical to the test specimens described in Section 3, geometries and welding technologies correspond with the same input data. The applied corrugation angles are 30°, 45° and 60° for the three specimens, respectively. A conventional I-girder with flat web is also analysed numerically as a reference specimen. All the specimens of S355 steel grade (material model of EN 1993-1-2:2005 [37] is used in the simulation) are fabricated with a length of 530 mm and a height of 280 mm, flanges are manufactured from steel plates with dimensions of 100 mm x 10 mm, while web thickness is 4 mm. The finite element models are shown in Figure 5.

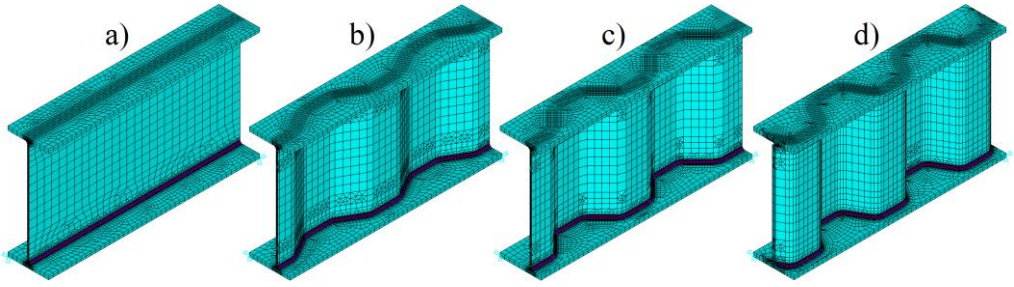

Figure 5: Finite element model of a) a conventional girder with I-shaped cross section and girders with corrugation angles of b) 30 °, c) 45 ° and d) 60 °.

Relatively fine mesh is used near the welds, while a coarser mesh is applied in regions far from the weld toe. Number of elements varies between 38000 - 50000 per specimens. Ambient temperature and initial temperature of the specimens are 20 °C, as measured during the manufacturing process. Girders are considered statically determinate in the mechanical analysis, that fits experimental set-up. 460 to 600 substeps are performed for the whole manufacturing process depending on trajectory lengths, cooling between weld passes and cooling to 20 °C to determine residual stresses. A sensitivity analysis is carried out to reveal the influence of corrugation angle, thermal efficiency (i.e., net heat input) and heat source model parameters. Thermal efficiency may be taken as 0.8 according to EN 1011-1:2009 [38] in case of metal active gas welding, however, Radaj [39] recommended a range between 0.65 and 0.9. Thus, thermal efficiency is modified in 0.05 steps in the range mentioned before to evaluate the effect of heat input. Nevertheless, 0.65 is considered to be the reference thermal efficiency to highlight the differences in net heat input. Reference heat source parameters are a = 5 mm, b = 2.5 mm, c_f = 2.5 mm, while c_r = 10 mm (see [10] for notations). The influence of heat source size and thus power density distribution is analysed using heat source parameter scaling. Scaling factors of 0.5, 1.0, 1.5 and 2.0 are chosen for all the characteristic parameters.

4.1.2 Residual stresses and geometric imperfections

Numerical results of the sensitivity analysis are presented in this section. The purpose is to demonstrate the evolution of total strains, typical deformations and residual stress distributions. First, the influence of corrugation angle is introduced. Figures 6-10 show the in-plane, out-of-plane and total deformations, longitudinal and von Mises residual stresses, respectively. These figures unambiguously demonstrate the beneficial effect of corrugated profiles regarding residual deformations. Total and out-of-plane deformations decrease as corrugation angle and effective depth of longitudinal (parallel) folds increase to resist bending moment about the longitudinal axis of the specimen due to angular distortion. Inclined folds and welding trajectories cross the neutral axis of the corrugated profile that leads to alternating movement of the heat source and eventually results in reduced deformations compared to the I-girder with flat web. Out-of-plane deformations are between -6.8 mm and 4.1 mm for the conventional I-girder, whilst it is reduced to -4.0 mm and 0.2 mm using a corrugation angle of 60°. Results also show that larger twisting distortions due to shear stresses may occur in case of conventional girders that could increase the need of corrections after welding. The comparison of global in-plane deformations also shows that a ‘waving’ pattern of local out-of-plane deformations is typical for the flanges of corrugated web girders (corresponds to a typical eigenshape [40] and measurements [25] as well) as the cold-formed profile grants some degree of restraint. However, the phenomenon results in extra bending moments about the neutral axis of the flange and thus additional stresses that leads to a non-uniform stress distribution in the flanges. Longitudinal and von Mises residual stresses are in the vicinity of yield strength near the welds in a representative cross section of a corrugated web girder, although, the assignation is not true for longitudinal stresses in the whole specimen as principle stress orientations unequivocally vary due to the corrugated web geometry. Compressive longitudinal residual stresses nearly reach the yield strength where the flange edge to web plate distance is smaller, while longitudinal stresses are compressive (top surface on upper flange/bottom surface on lower flange) and tensile (bottom surface on upper flange/top surface on lower flange) as well on the other side of the web. Conventional I-girders may be characterized by quasi-stationary residual stress distribution, except near the ends of the specimen. Quasi-zero welding-induced residual stresses evolve in the corrugated webs due to the negligible axial stiffness (i.e., ‘accordion effect’), while mainly compressive longitudinal residual stresses appear in the flat web. It is in accordance with the tendency taken into account in standards and presented in the international literature.

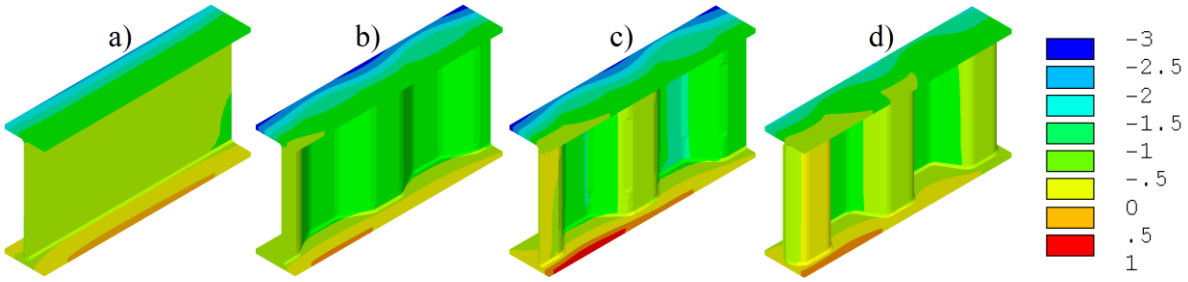

Figure 6: In-plane deformations of a) a conventional girder with I-section and girders with corrugation angles of b) 30°, c) 45° and d) 60°.

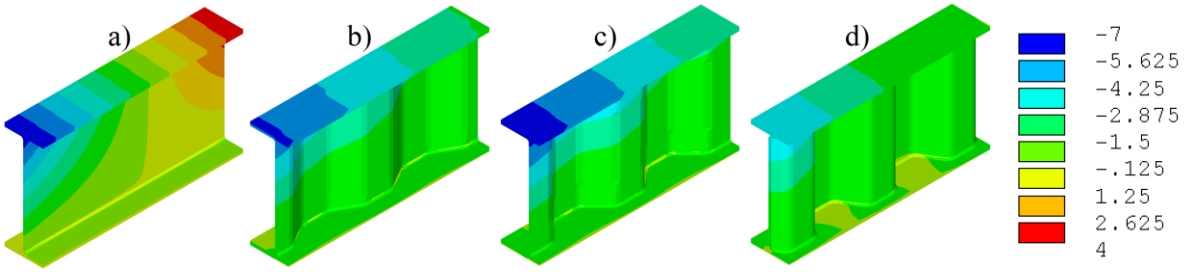

Figure 7: Out-of-plane deformations of a) a conventional girder with I-section and girders with corrugation angles of b) 30°, c) 45° and d) 60°.

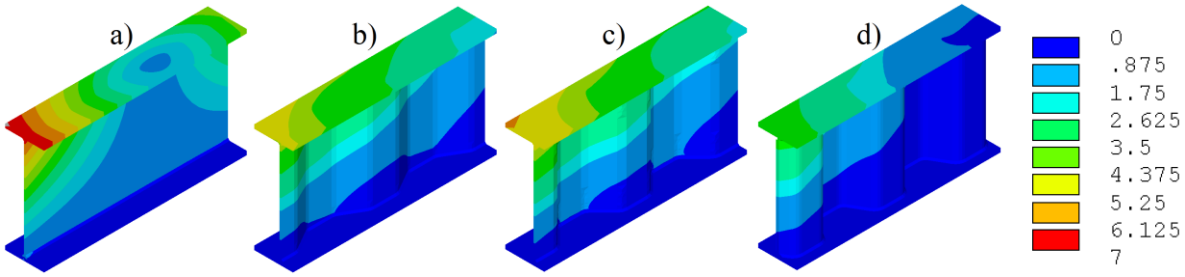

Figure 8: Total deformations of a) a conventional girder with I-section and girders with corrugation angles of b) 30°, c) 45° and d) 60°.

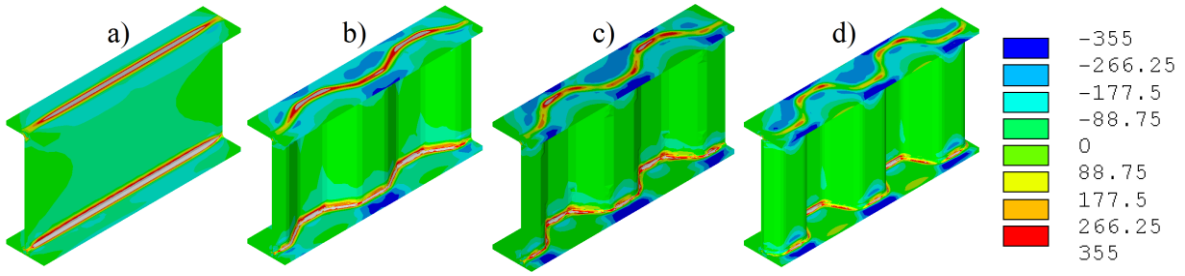

Figure 9: Longitudinal residual stresses of a) a conventional girder with I-section and girders with corrugation angles of b) 30°, c) 45° and d) 60°.

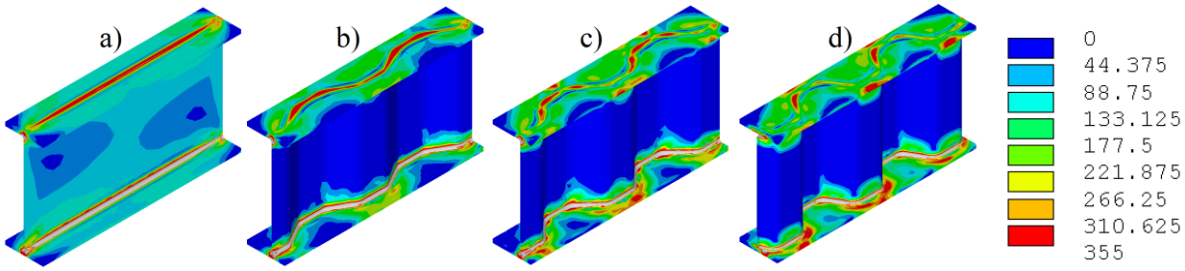

Figure 10: von Mises residual stresses of a) a conventional girder with I-section and girders with corrugation angles of b) 30°, c) 45° and d) 60°.

The temporal evolution of total strains, which is the sum of elastic and thermal strains in an elastic region neglecting creep effects is discussed for the investigated corrugation angles, heat source model parameters and thermal efficiencies (i.e., net heat input). Nodes are selected representing strain gauges on both sides of the web ('Side I' and 'Side II') according to the experimental set-up. Longitudinal residual stress (σ_z) distributions in the web (on 'Side I' and 'Side II' surfaces) and in the flanges (on 'Top' and 'Bottom' surfaces plus in the 'Neutral' plane of the plates) are demonstrated for all the analysed cases in a characteristic cross section (midsection of the specimens). Longitudinal stresses in upper and lower flanges are averaged for representation purposes as flanges are identical and the specimens are symmetric. Nodes for time-history post-processing, the analysed cross section for residual stress evaluation and an example of von Mises residual stresses due to lack of fusion are shown in Figure 11.

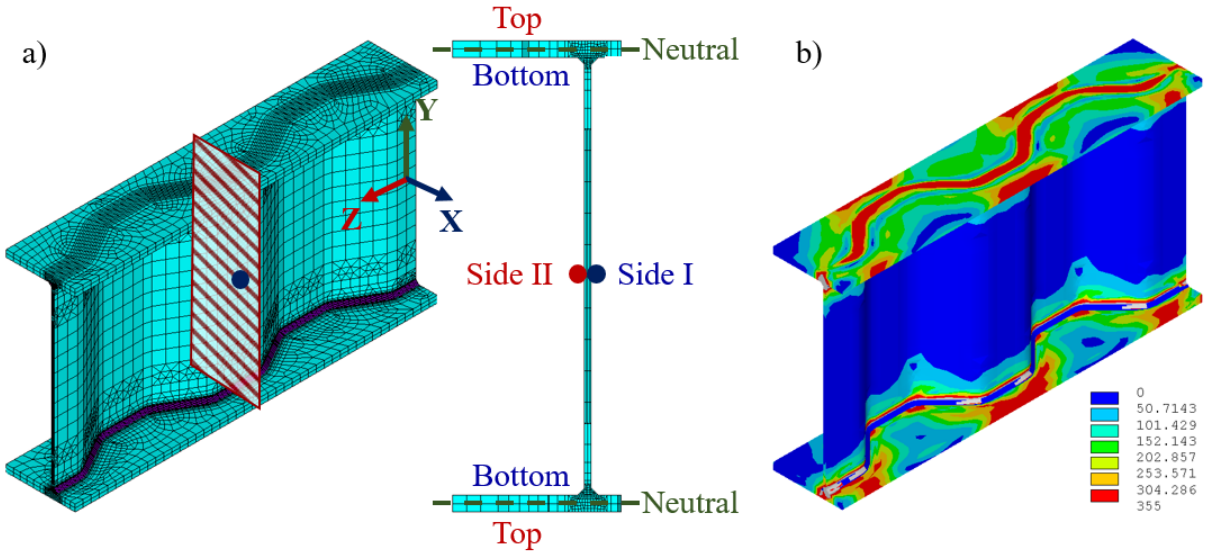

Figure 11: a) Cross sections for residual stress evaluation and selected nodes for time-history post-processing, b) von Mises residual stresses due to lack of fusion.

Total strains for the I-girder with flat web and configurations with different corrugation angles are shown in Figure 12. The bending moment about the longitudinal axis of the specimen due to angular distortion results in non-uniform elastic strain distribution (compressive and tensile residual strains as well in the range of -100 and 100 μm/m) in the web of corrugated web girders, while its influence on girders with flat web is negligible (only compressive residual strains with a magnitude of around -245 μm/m). The ratio of compressive to tensile residual strains is around 1.0 regarding absolute values for corrugated web girders. A delay in total strain peaks can be recognized due to distinct welding trajectory and cooling phase lengths between weld passes. Results of heat source parameter scaling are presented in Figure 13 for the girder with corrugation angle of 45° showing that within the range of 0.5 and 1.5, variance in total strains is negligible regarding the selected nodes. Scaling factor of 2.0 results in low power density and thus relatively low temperatures in the weld bead. The technique used for addition of material results in lack of fusion (Figure 11) as temperature does not reach the reference temperature. Obviously, quasi-zero stresses in the weld bead has an effect on residual stresses in the web in conjunction with obtaining equilibrium of resultant internal forces and bending moments in any section of the specimen. Results of thermal efficiency variation are presented in Figure 14. In the range of 0.65 and 0.9, maximum variances of 90 μm/m and 95 μm/m in total strains turned up during welding on Side I and Side II, respectively. Thermal strains disappear as a result of cooling, thus, residual strains are elastic for the analysed nodes.

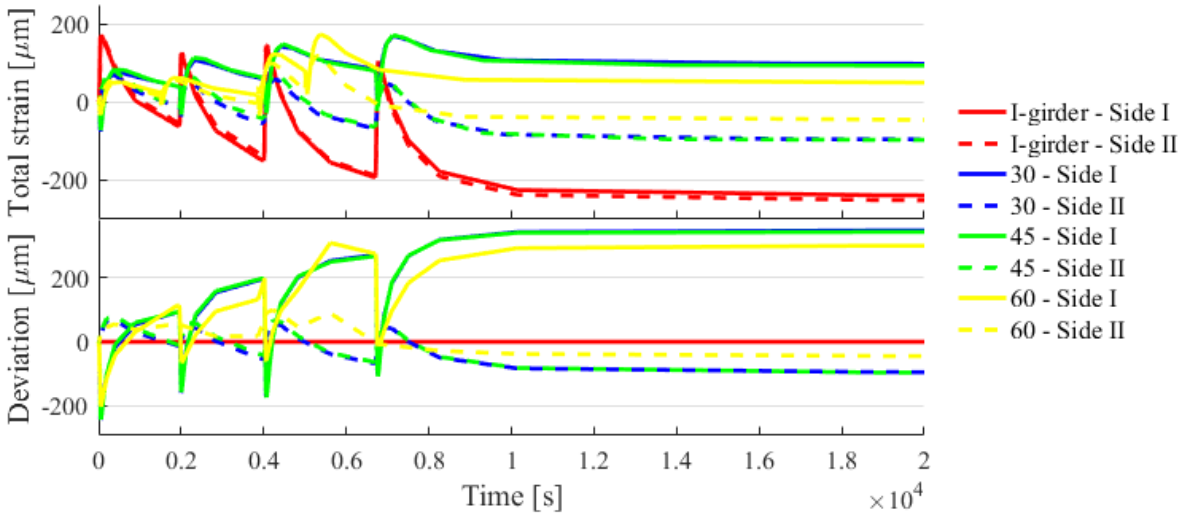

Figure 12: Evolution of total strains in time using different corrugation angles. The conventional I-girder with flat web is taken as reference for total strain deviation calculations.

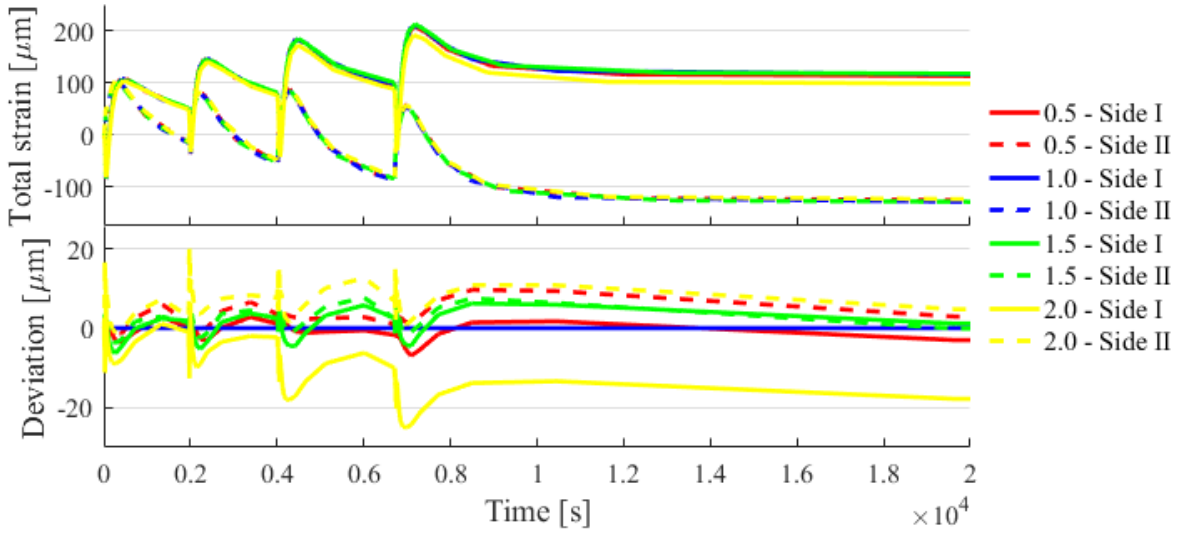

Figure 13: Evolution of total strains in time using different heat source parameters. Scaling factor of 1.0 is taken as reference for total strain deviation calculations.

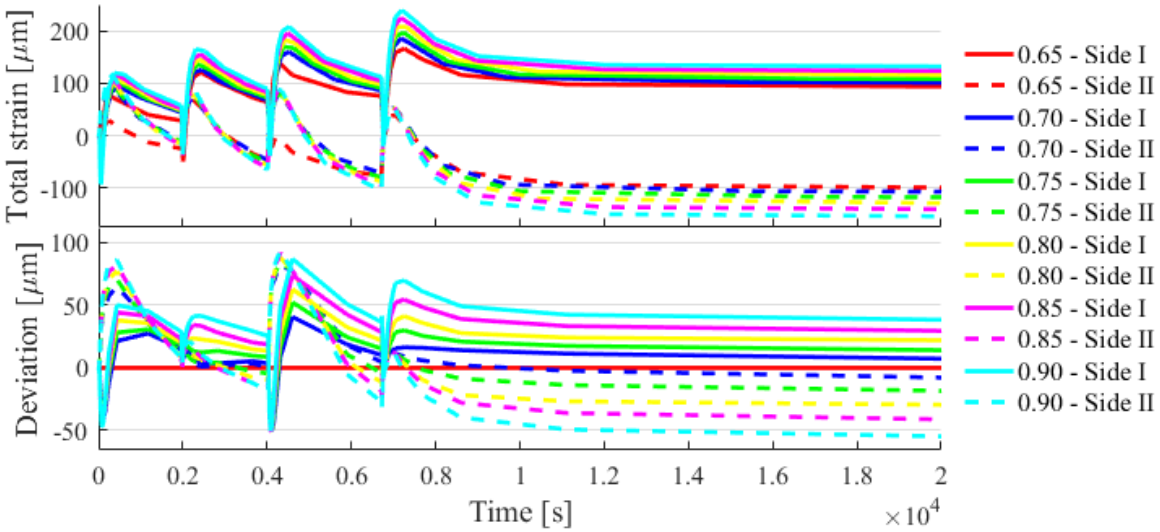

Figure 14: Evolution of total strains in time using different thermal efficiencies. Thermal efficiency of 0.65 is taken as reference for total strain deviation calculations.

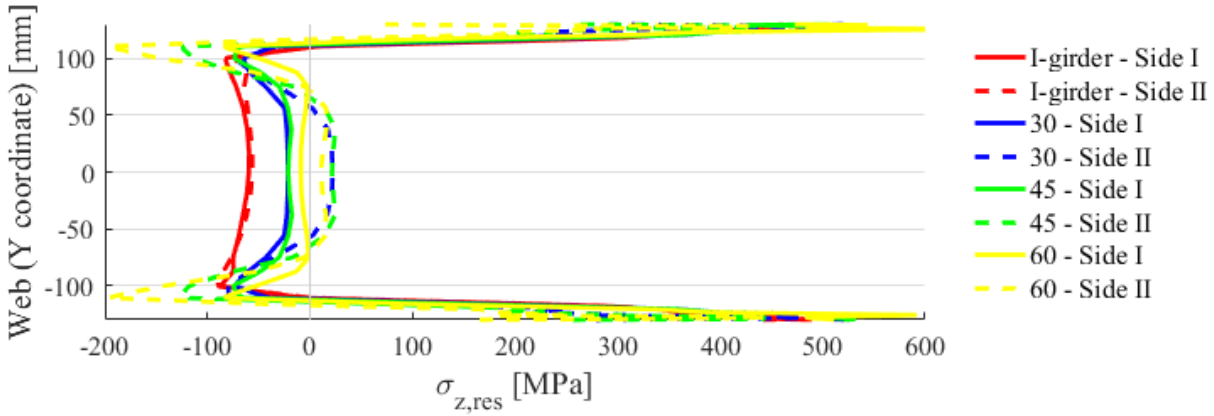

Figure 15: Longitudinal residual stress distribution in the web using different corrugation angles.

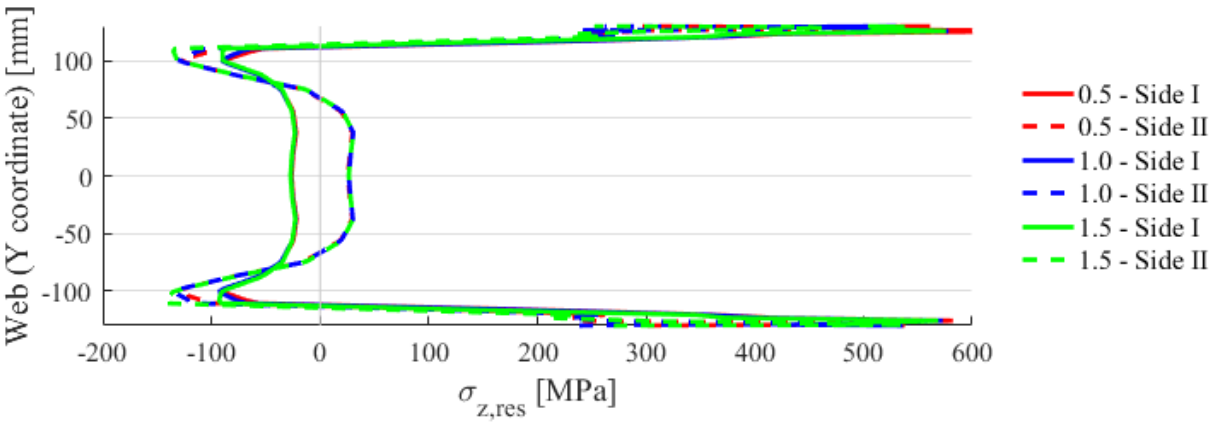

Figure 16: Longitudinal residual stress distribution in the web using different heat source parameter scaling (corrugation angle is 45°).

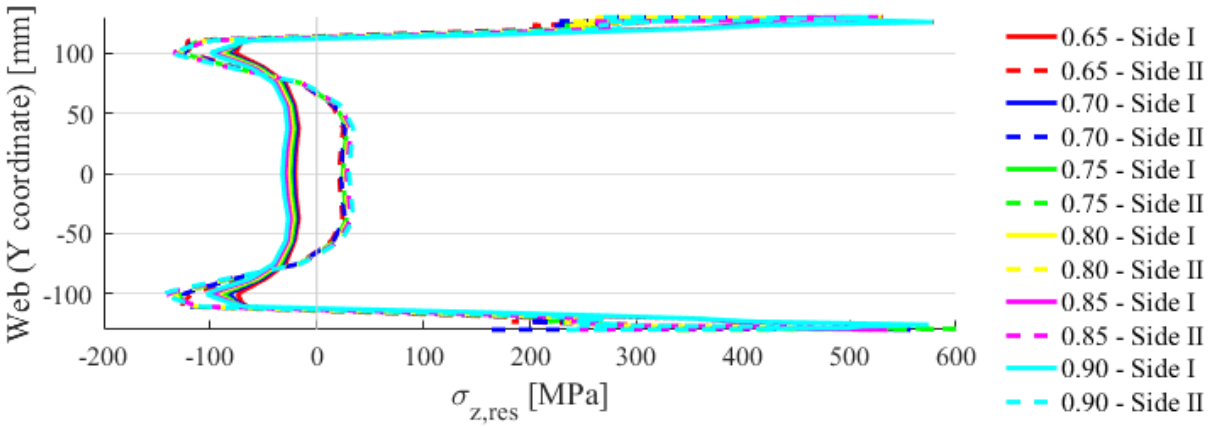

Figure 17: Longitudinal residual stress distribution in the web using different thermal efficiencies (corrugation angle is 45°).

Longitudinal residual stresses due to welding in the web for the I-girder with flat web and configurations with different corrugation angles, heat source model parameters and thermal efficiencies (i.e., net heat input) are shown in Figures 15-17. Heat source parameter scaling factor of 2.0 is not taken into account in the longitudinal residual stress evaluation as the results are incorrect due to lack of fusion. The sizes of tensile zones near the weld are nearly the same (~15-20 mm→~4-5 t_w web thickness) for all the investigated cases, even for the I-girder with flat web. Significant compressive residual stress peaks (~70-200 MPa) appear around 20-25 mm (~5-6 t_w web thickness) from the joint of the web and the flange. However,

nearly zero (~5-30 MPa) compressive and tensile stresses are present in the middle of the web for corrugated web girders, while only compressive stresses (~ 60 MPa) are typical in this region for the I-girder. Corrugation angle, thermal efficiency and cross sectional dimensions in general may have a large influence on residual stresses in the web, as observed in the current research program.

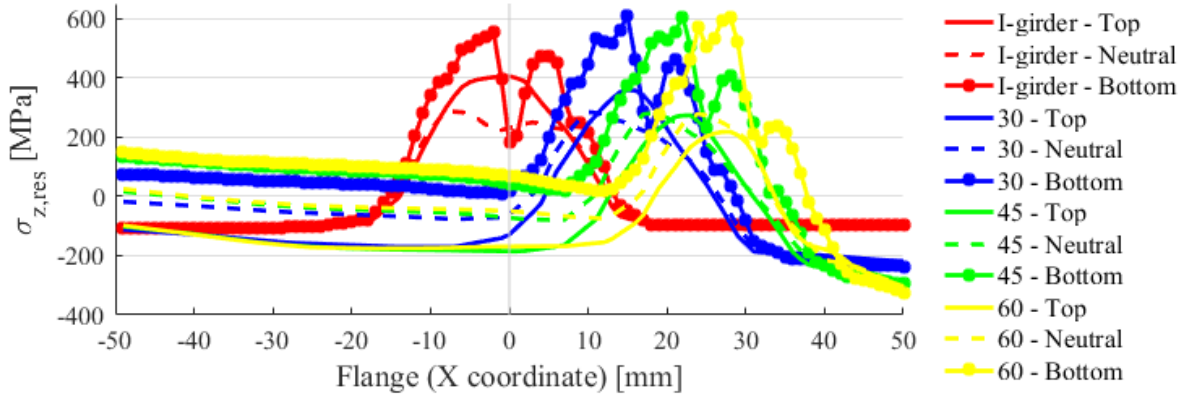

Figure 18: Averaged longitudinal residual stress distribution in the flanges using different corrugation angles.

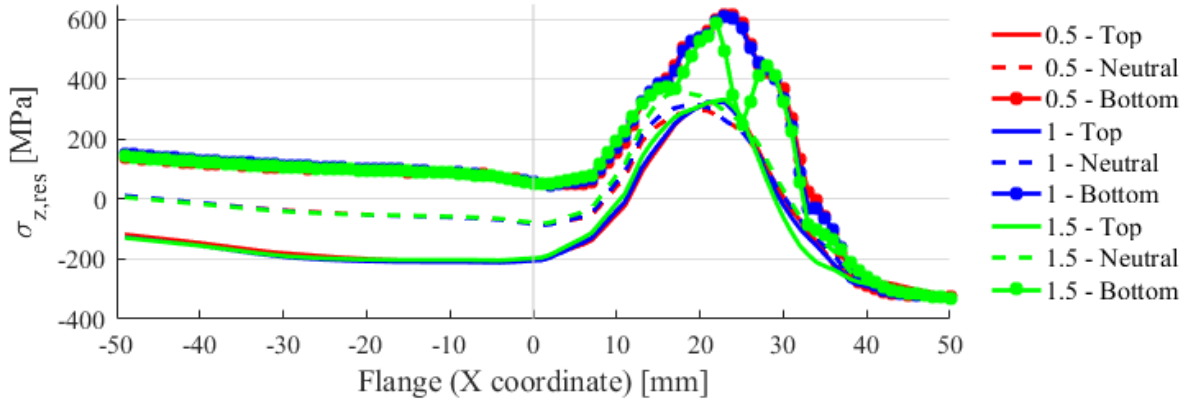

Figure 19: Averaged longitudinal residual stress distribution in the flanges using different heat source parameter scaling (corrugation angle is 45°).

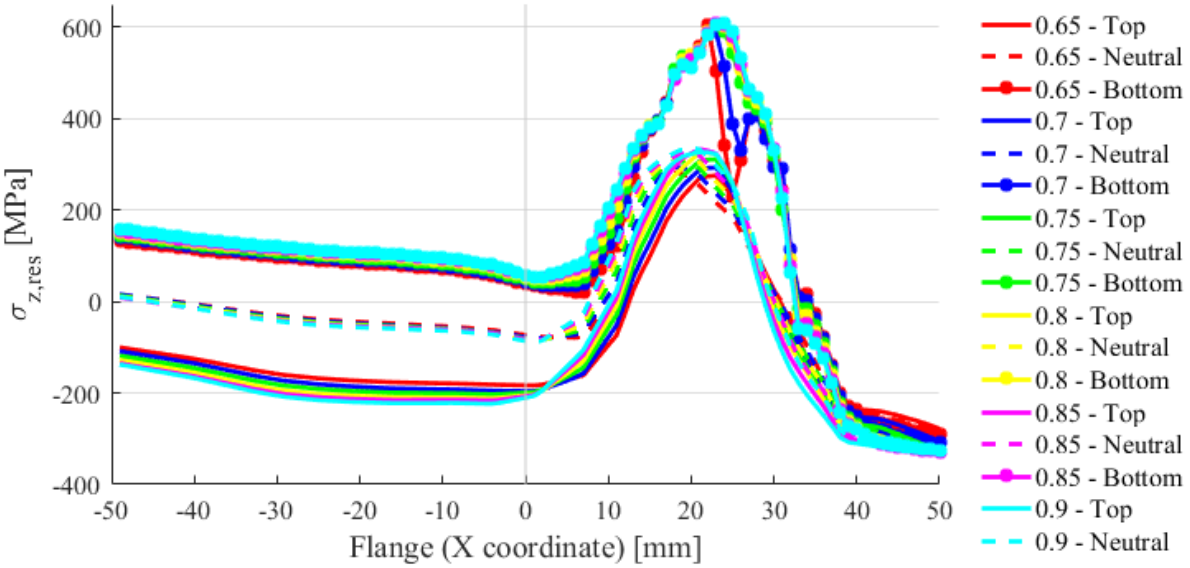

Figure 20: Averaged longitudinal residual stress distribution in the flanges using different thermal efficiencies (corrugation angle is 45°).

Averaged longitudinal residual stresses due to welding in the flanges (flanges are assumed to be identical) for the I-girder with flat web and configurations with different corrugation angles, heat source model parameters and thermal efficiencies (i.e., net heat input) are shown in Figures 18-20. The magnitude of compressive stresses is ~90-100 MPa in the flanges for the I-girder. The variation of corrugation angle results in the shift of maximum tensile residual stresses as the plane of the subpanel is getting closer to the edge of the flange as corrugation angle increases. Its influence on the tensile residual stress magnitude is negligible, however, welding-induced bending moment results in compressive (~ 100 MPa) and tensile stresses (max.~ 180 MPa) on the surfaces further from the web ('Side I'). Compressive stresses increase, almost reaching the yield strength, while corrugation angle increases on the other side of the web ('Side II'). The sizes of tensile zones near the weld are nearly the same (~25-28 mm→~2.5-2.8 t_f flange thickness) for all the investigated cases, even for the I-girder with flat web. In case of scaling factor of 1.5 a decrease in tensile residual stresses can be observed in the plane of the web due to lower power density and temperature. The variation of heat input, in the range of 0.65-0.90 thermal efficiencies, results in max. ~10 % change in tensile and compressive residual stresses far from the web ('Side I') and max. ~30 % variation in compressive stresses on 'Side II'. Corrugation angle, thermal efficiency and cross sectional dimensions in general may have a large influence on residual stresses in the flanges as well. Generally, it can be observed, that welding results in mainly membrane-type residual stresses in case of flat web girders. However, bending-type residual stresses are dominant in case of corrugated web girders, and axial membrane residual stresses are significantly smaller in the web. Additional transverse bending moment can be also obtained in flanges in case of corrugated web girders, which is also a specialty of these girder types. Corrugated profile results in asymmetric residual stress pattern within the cross sections, while increase in the corrugation depth results in larger bending-type residual stresses.

4.1.3 Verification

The verification of the developed numerical model for welding simulation of corrugated web girders is presented in this section. Figure 21 shows the total strains measured by strain gauges ('Exp') and computed results using finite element method ('FEM') at the position shown in Figure 11 on 'Side I'. The comparison of experimental and numerical data shows good agreement for all the three analysed corrugation angles (30°, 45° and 60°). The effect of different heat source parameters and heat inputs on total strains has been introduced previously. Heat source parameters, except in case of lack of fusion, do not have a large influence (maximum of 10 μm/m), while 25 % change in heat input could result in 90 μm/m variance in total strains. The maximum difference is observed for corrugation angle of 60°, which is 80 μm/m and it is within the tolerance according to the sensitivity analysis.

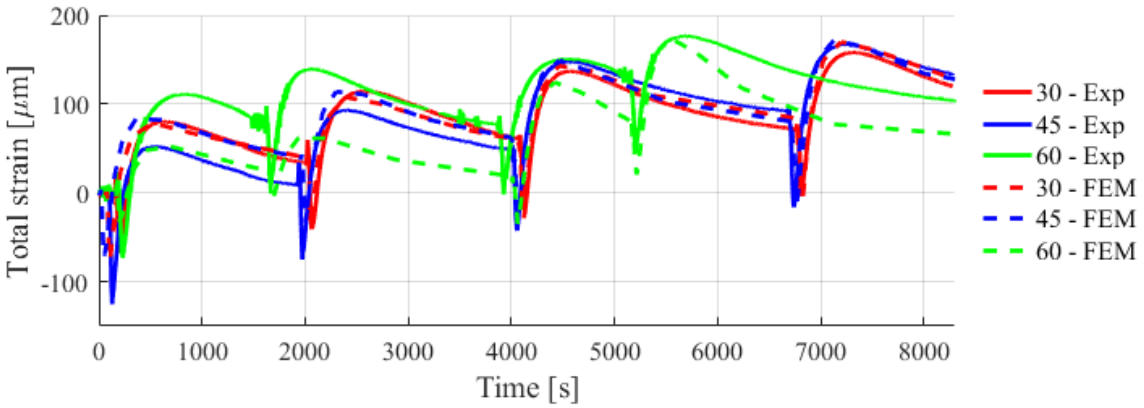

Figure 21: Evolution of total strains based on measurements ('Exp') and simulation ('FEM').

4.2 Geometrical and material nonlinear analysis with imperfections

4.2.1 Background of simulation

The background of performing a geometrical and material nonlinear analysis with imperfections (GMNIA) is described in EN 1993-1-5:2005 [28] for plated structural elements. Generally, the standard recommends to use local and global equivalent geometric imperfections, which include the effect of residual stresses and geometric imperfections due to manufacturing. The numerical approach used for investigating stability problems of virtually manufactured specimens has been already presented in [9] and [11] for flexural buckling of columns and local buckling of stub columns with welded box sections, respectively. The material model for the welding simulation and the GMNIA is a multilinear isotropic hardening model proposed in EN 1993-1-2:2005 [37]. Large deflection effects are also included in the analysis. The approach can be divided into five steps: (i) welding simulation, (ii) mapping and defining initial state variables (i.e., residual stresses, strains and accumulated equivalent plastic strain) node-by-node regarding the results of the welding simulation, (iii) updating the geometry of the finite element model to the deformed configuration in accordance with results of the welding simulation, (iv) definition of loads and boundary conditions during virtual testing, (v) force/displacement controlled loading.

4.2.2 Virtual testing

The developed approach for virtual testing is illustrated with an example below in Figure 22. Details shown in the figure correspond to the current analyses. Transverse stiffeners at the supports and in the plane of loading are modelled with rigid regions. The following geometries are investigated (t_w = 4 mm, h_w = 530 mm, t_f = 10 mm, b_f = 100 mm for all the cases) with a total length of 1060 mm and S355 steel grade: a) conventional I-girder, b-d) corrugated web girders with θ = 30°, 45° and 60°, respectively with a_1 = a_2 = 40 mm. Heat input is in agreement with the one applied in the sensitivity analysis, while travel speed is 10 mm/s in the welding simulation.

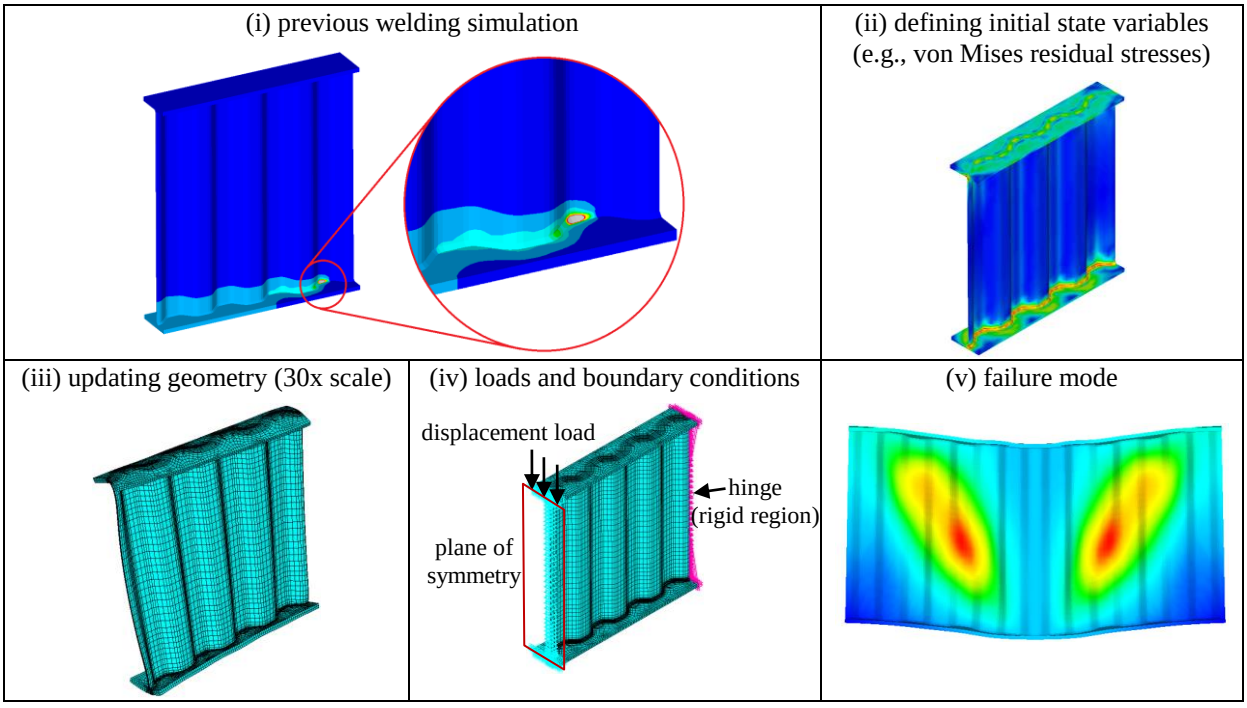

Figure 22: Steps of the developed approach for virtual testing of specimens undergoing virtual manufacturing.

4.2.3 Shear buckling strength

The influence of virtual manufacturing and thus welding-induced deformations and residual stresses on shear buckling strength of a conventional I-girder with flat web and corrugated web girders is presented in this section. In addition, shear buckling strength is also determined using equivalent geometric imperfections. Local out-of-plane imperfections are applied with a magnitude of $h_w/200$ corresponding to the first eigenshape (plate buckling) using linear buckling analysis. Failure modes, in the case of virtual manufacturing, and reaction force (shear force) - displacement curves of the investigated geometries are shown in Figure 23.

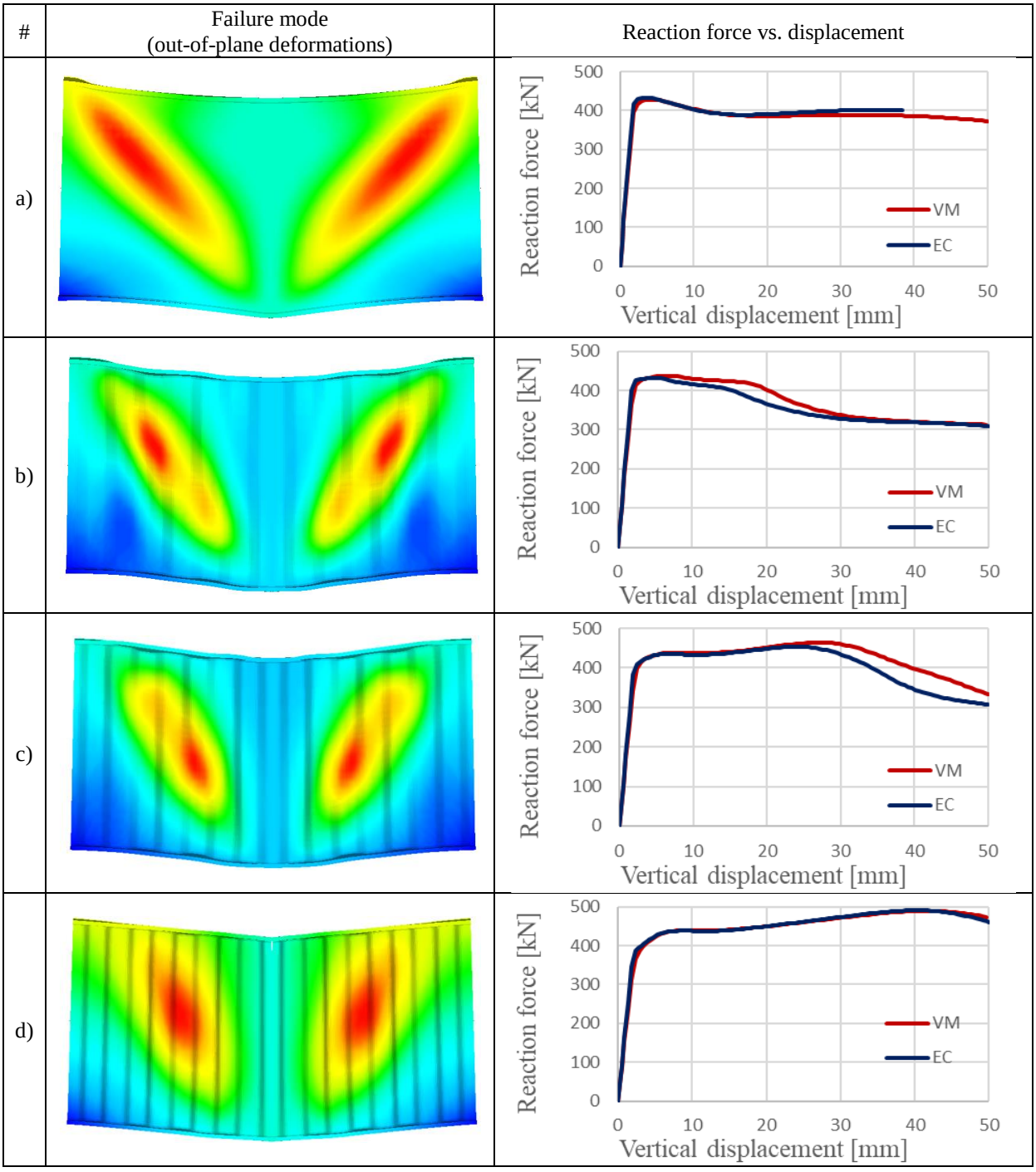

Figure 23: Failure modes and and reaction force – displacement curves for the investigated specimens (VM – virtual manufacturing, EC – Eurocode).

The calculated shear buckling strengths using equivalent geometric imperfections ($h_w/200$) and the virtual testing of a previously manufactured specimen are in good agreement for the selected geometries as it is shown in the load – displacement curves presented in Figure 23. Increasing the corrugation angle results in higher shear buckling strength and larger ultimate vertical displacement. Shear buckling strength varies between 427.8 kN and 490.2 kN, while the corresponding ultimate vertical displacement is between 4.4 mm and 41.2 mm. Plastic shear buckling failure mode is specific for the investigated specimens as the pure shear resistance of the web is 434.5 kN assuming that shear stress is equal to the shear yield strength. The applicability of equivalent geometric imperfections recommended by EN 1993-1-5:2006 is presented for the investigated geometries, however, an extended research program is necessary to evaluate the application limits.

5 CONCLUSION

The aim of the current research program is to (i) perform an experimental and numerical study focusing on residual stress distribution in corrugated web girders, (ii) verify the developed finite element model for welding simulation, (iii) determine and compare the typical welding-induced longitudinal residual stress distributions in the web and in flanges as well, (iv) comparison of the residual stress pattern in corrugated web girders and in conventional I-girders with flat web and (v) to apply virtual manufacturing, i.e., welding simulation, as an input supplying residual stresses and deformations for subsequent virtual testing and the determination of shear buckling resistance. The results showed that the residual stress distribution for corrugated web girders and conventional I-girders with flat web differs in a great extent. Mainly membrane-type residual stresses are typical for girders with flat web, except in case of thick plates, while bending-type residual stresses dominate for corrugated web girders. Membrane residual stresses are negligible in the web for corrugated web girders, except in the vicinity of the weld, nevertheless, notable compressive residual stresses may evolve in the web of an I-girder with flat web. The developed finite element model for welding simulation of corrugated web girders is verified with strain gauge measurements during welding, while uncertainties in welding variables, heat source models and the influence of corrugation angle are analysed and discussed in the paper. Welding simulation become an ultimate tool for virtual testing of virtually manufactured conventional I-girders and corrugated web girders. In addition, shear buckling strengths of simulated specimens are determined using virtual testing as well as the approach recommended by EN 1993-1-5:2006. The numerical results show that the equivalent geometric imperfection with a magnitude of $h_w/200$ is applicable for the investigated geometries, however, an extended research program is necessary to evaluate the application limits.

REFERENCES

[1] El Hadidy A.M., Hassanein M.F. and Zhou M., "The effect of using tubular flanges in bridge girders with corrugated steel webs on their shear behaviour – A numerical study", *Thin-Walled Structures*, **124**, 121–135, 2018.

[2] Bergfelt A. and Leiva L., "Buckling of trapezoidally corrugated webs and panels", *IABSE reports*, 67–74, 1986.

[3] Luo R. and Edlund B., "Shear capacity of plate girders with trapezoidally corrugated webs", *Thin-Walled Structures*, **26**, 19–44, 1996.

[4] Luo R. and Edlund B., "Buckling Analysis of Trapezoidally Corrugated Panels Using Spline Finite Strip Method", *Thin-Walled Structures*, **18**, 209–224, 1994.

[5] Zevallos E., Hassanein M.F., Real E. and Mirambell E., "Shear evaluation of tapered bridge

girder panels with steel corrugated webs near the supports of continuous bridges", *Engineering Structures*, **113**, 149–159, 2016.

[6] Hassanein M.F. and Kharoob O.F., "Shear buckling behavior of tapered bridge girders with steel corrugated webs", *Engineering Structures*, **74**, 157–169, 2014.

[7] Guo T. and Sause R., "Analysis of local elastic shear buckling of trapezoidal corrugated steel webs", *Journal of Constructional Steel Research*, **102**, 59–71, 2014.

[8] Hassanein M.F., Elkawas A.A., El Hadidy A.M. and Elchalakani M., "Shear analysis and design of high-strength steel corrugated web girders for bridge design", *Engineering Structures*, **146**, 18–33, 2017.

[9] Kollár D. and Kövesdi B., "Experimental and numerical simulation of welded columns", *Zavarivanje – Welding Proceedings*, 123–132, 2016.

[10] Kollár D. and Kövesdi B., "Numerical Simulation of Welding Process", *Young Welding Professionals International Conference, YPIC2015*, Budapest, 6, 2015.

[11] Kollár D., Kövesdi B. and Néző J., "Numerical simulation of welding process – Application in buckling analysis", *Periodica Polytechnica Civil Engineering*, **61**(1)**,** 9257, 2017.

[12] Somodi B., Kollár D., Kövesdi B., Néző J. and Dunai L., "Residual stresses in high-strength steel welded square box sections", *Proceedings of the Institution of Civil Engineers: Structures and Buildings*, **170**(11), 9, 2017.

[13] Nagaraja N.R., Estuar F.R. and Tall L., "Residual stresses in welded shapes", *Welding Journal*, **43**(7), 295s–306s, 1964.

[14] Alpsten G.. and Tall L., "Residual Stresses in Heavy Welded Shapes", *Welding Journal*, **39**(3), 93s–105s, 1970.

[15] Beg D. and Hladnik L., "Slenderness limit of class 3 I cross-sections made of high strength steel", *Journal of Constructional Steel Research*, **38**(3), 201–217, 1996.

[16] Chernenko D.E. and Kennedy D.J.L., "An analysis of the performance of welded wide flange columns", *Canadian Journal of Civil Engineering*, **18**(4), 537–555, 1991.

[17] Ban H.Y., Shi G. and Shi Y.J., "Experimental and unified model investigations on residual stress within high strength steel welded I-sections", *Engineering Mechanics*, **31**(8), 83–91, 2014.

[18] Liu X. and Chung K.F., "Eerimental investigation into residual stresses of welded H-sections made of Q690 steel materials", *The 14th East Asia-Pacific Conference on Structural Engineering and Construction*, 2016.

[19] Zhu Q., Nie S., Yang B., Xiong G. and Dai G., "Experimental Investigation on Residual Stresses in Welded Medium-Walled I-shaped Sections Fabricated from Q460GJ Structural Steel Plates", *International Journal of Structural and Construction Engineering*, **11**(11), 1428–1437, 2017.

[20] European Convention for Constructional Steelworks. Manual on Stability of Steel Structures: Part 2.2. Mechanical properties and residual stresses, 1976.

[21] BSK 99. Swedish design rules for steel structures, 2003.

[22] Code for Design of Steel Structures Committee. Application Construal of Code for Design of Steel Structures in China (in Chinese), 2003.

[23] Wang Y.B., Li G.Q. and Chen S.W., "The assessment of residual stresses in welded high strength steel box sections", *Journal of Constructional Steel Research*, **76**, 93–99, 2012.

[24] Pasternak H. and Kubieniec G., "Plate girders with corrugated steel webs", *Journal of Civil Engineering and Management*, **16**(2), 166–171, 2010.

[25] Jáger B., Dunai L. and Kövesdi B., "Flange buckling behavior of girders with corrugated web Part I: Experimental study", *Thin-Walled Structures*, **118**, 181–195, 2017.

[26] Lho S.H., Lee C.., Oh J.T., Ju Y.K. and Kim S.D., "Flexural Capacity of Plate Girders with Very Slender Corrugated Webs", *International Journal of Steel Structures*, **14**(4), 731–744, 2014.

[27] Moon J., Lim N.H. and Lee H.E., "Moment gradient correction factor and inelastic flexural-

torsional buckling of I-girder with corrugated steel webs", *Thin-Walled Structures*, **62**, 18–27, 2013.

[28] EN 1993-1-5:2006. Eurocode 3: Design of steel structures – Part 1-5: Plated structural elements, 2006.

[29] Galambos T.V., *Guide to Stability Design Criteria for Metal Structures*, John Wiley & Sons, Inc., 1998.

[30] Easley J.T., "Buckling formulas for corrugated metal shear diaphragms", *Journal of the Structural Division*, **101**, 1403–1417, 1975.

[31] El-Metwally A.S., *Prestressed composite girders with corrugated steel webs*, MSc, University of Calgary, 1998.

[32] Driver R.G., Abbas H.H. and Sause R., "Shear Behavior of Corrugated Web Bridge Girders", *Journal of Structural Engineering*, **132(2),** 195–203, 2006.

[33] Yi J., Gil H., Youm K. and Lee H., "Interactive shear buckling behavior of trapezoidally corrugated steel webs", *Engineering Structures*, **30**(6), 1659–1666, 2008.

[34] Sause R. and Braxtan T.N., "Shear strength of trapezoidal corrugated steel webs", *Journal of Constructional Steel Research*, **67**(2), 223–236, 2011.

[35] Leblouba M., Junaid M.T., Barakat S., Altoubat S. and Maalej M., "Shear buckling and stress distribution in trapezoidal web corrugated steel beams", *Thin-Walled Structures*, **113**, 13–26, 2017.

[36] Leblouba M., Barakat S., Altoubat S., Junaid T.M. and Maalej M., "Normalized shear strength of trapezoidal corrugated steel webs", *Journal of Constructional Steel Research*, **136**, 75–90, 2017.

[37] EN 1993-1-2:2005. Eurocode 3: Design of steel structures – Part 1-2: General rules –Structural fire design, 2005.

[38] EN 1011-1:2009. Welding - Recommendations for welding of metallic materials - Part 1: General guidance for arc welding, 2009.

[39] Radaj D., *Heat Effects of Welding: Temperature Field, Residual Stress, Distortion*, 1992. doi:10.1007/978-3-642-48640-1.

[40] Jáger B., Kövesdi B. and Dunai L., "Flange buckling resistance of trapezoidal web girders: Experimental and numerical study", *ce/papers*, **1**(2-3), 4088–4097, 2017.